

Technical Communication

Citation

Cardoso LHD, Doerrier C, Gnaiger E (2021)
Magnesium Green for fluorometric measurement of ATP production does not interfere with mitochondrial respiration. Bioenerg Commun 2021.1.
doi:10.26124/bec:2021-0001

Author contributions

LHDC, CD and EG designed the work; LHDC collected and analyzed data and drafted the article; CD and EG critically revised the article, all authors approved the final version of the manuscript.

Conflicts of interest

EG is founder and CEO of Oroboros Instruments, Innsbruck, Austria.

Academic editor

Chinopoulos Christos, Semmelweis University, HU

Received 2021-02-11

Reviewed 2021-05-05

Resubmitted 2021-06-25

Accepted 2021-06-28

Published 2021-06-30

Editorial and peer review record

[doi:10.26124/bec:2021-0001](https://doi.org/10.26124/bec:2021-0001)

Preprint

MitoFit Preprints 2021.1
[doi:10.26124/mitofit:2021-0001](https://doi.org/10.26124/mitofit:2021-0001)

Data availability

Original files are available Open Access at Zenodo repository:
[10.5281/zenodo.4916141](https://doi.org/10.5281/zenodo.4916141)

Magnesium Green for fluorometric measurement of ATP production does not interfere with mitochondrial respiration

 Luiza HD Cardoso*,  Carolina Doerrier,  Erich Gnaiger

Oroboros Instruments, Innsbruck, Austria

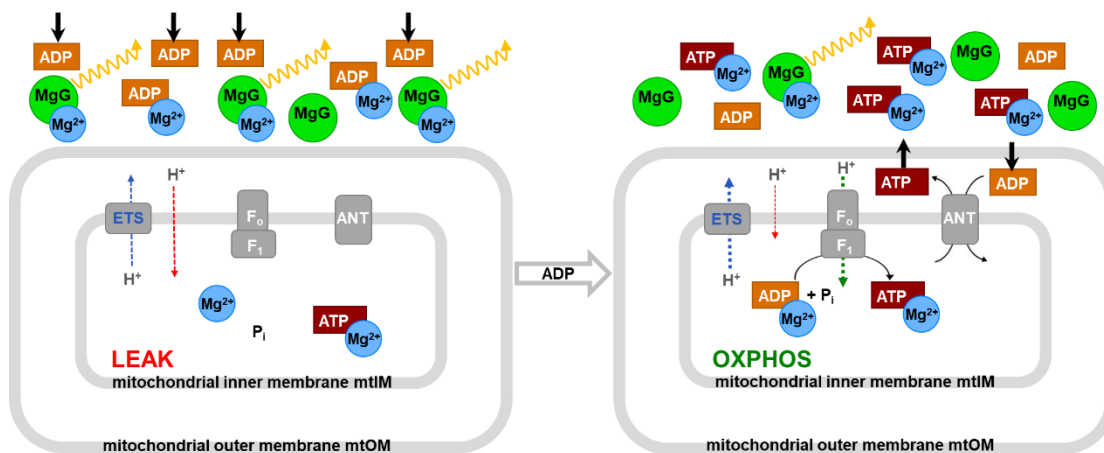
*Corresponding author: luiza.cardoso@orooboros.at

BEC 2021.1. [doi:10.26124/bec:2021-0001](https://doi.org/10.26124/bec:2021-0001)

Abstract

For the advanced study of mitochondrial function, high-resolution respirometry is extended by fluorometric measurement of ATP production using the fluorophore Magnesium Green™ (MgG). A common problem with several fluorescent dyes is the inhibition of mitochondrial respiration. In the present study, a coupling control protocol was applied in combination with MgG to measure ATP production simultaneously with respiration for calculation of $P_{\text{O}_2}/\text{O}_2$ ratios. MgG at 1.1 μM did not affect respiration through the NADH-linked and succinate-linked pathways. Respiration was not inhibited in any of the coupling control states, hence coupling control efficiencies were not affected by MgG.

Keywords – ATP production; high-resolution respirometry HRR; Magnesium Green MgG; mitochondria mt; oxidative phosphorylation OXPHOS; fluorometry; FluoRespirometry



Graphical abstract - Concept of the MgG assay according to Chinopoulos et al (2014). MgG fluoresces when bound to Mg²⁺. ADP and ATP compete for Mg²⁺ binding with different affinities; ATP has a higher affinity for Mg²⁺ compared to ADP. When ADP is added and binds a large fraction of free Mg²⁺, MgG fluorescence drops sharply. During subsequent oxidative phosphorylation ADP is phosphorylated to ATP, which is exchanged for ADP by the adenine nucleotide translocase ANT. Extramitochondrial ATP increases, more Mg²⁺ is bound to ATP, and MgG fluorescence decreases further. This decline is analyzed as ATP production. MgG does not impair mitochondrial respiratory control.

1. Introduction

Mitochondrial ATP production can be analyzed with a fluorometric technique using Magnesium Green™ (MgG) as a fluorescent probe, as described by Chinopoulos et al (2009). Application of the Mg²⁺-sensitive fluorophore as an indicator of ATP production relies on the fact that ADP and ATP have different affinities for Mg²⁺ (Gnaiger, Wyss 1994; Leysens et al 1996; Budinger et al 1998). ADP is phosphorylated to ATP in the mitochondrial matrix. In the phosphorylation system ADP/ATP and inorganic phosphate P_i are exchanged stoichiometrically by the adenine nucleotide translocase ANT and the phosphate carrier PiC. Under experimental conditions when ADP decreases while ATP increases in the extramitochondrial milieu, the Mg²⁺ concentration declines due to the higher affinity for Mg²⁺ of ATP than ADP. Therefore, the fluorometric assay with the membrane-impermeant MgG provides a quantitative approach to analyze mitochondrial ATP production. This method was developed further to measure concomitantly mitochondrial ATP production and O₂ consumption in the Oroboros O2k-FluoRespirometer which is an experimental system complete for high-resolution respirometry including fluorometry (Chinopoulos et al 2014).

Fluorescent dyes are widely used to assess various parameters relevant in mitochondrial physiology. Safranin, rhodamine and its derivatives, such as TMRM, are frequently employed as reporters of the mitochondrial membrane potential $\Delta\Psi_{p+}$. However, all $\Delta\Psi_{p+}$ dyes have been shown to affect mitochondrial respiration (Scaduto, Grotyohann 1999). Like TPP⁺, safranin mainly affects the NADH (N)-linked pathway, the phosphorylation system, and to a smaller extent the succinate (S)-linked pathway

(Krumshabel et al 2014). The effect of $\Delta\Psi_p$ fluorescent probes can be explained since they accumulate in the mitochondrial matrix and thus possibly affect mitochondrial function.

Amplex UltraRed is frequently employed in mitochondrial physiology studies to analyze H_2O_2 production. This dye was shown to affect mitochondrial respiration, even though the mitochondrial membranes are not permeable to this fluorophore (Makrecka-Kuka et al 2015). Therefore, it is important to analyze whether MgG affects mitochondrial respiration, despite the fact that mitochondrial membranes are not permeable to this fluorophore.

In the present technical communication, we report the effect of MgG on mitochondrial respiration, providing an important contribution for the applicability of the MgG assay for analysis of P_{O_2}/O_2 ratios in mitochondrial preparations. The experimental MgG concentration was chosen for simultaneous assessment of ATP production and mitochondrial respiration, which is the gold standard to evaluate mitochondrial function. Coupling control protocols using NADH- and succinate-linked substrates showed that mitochondrial respiration was not affected by MgG in LEAK, OXPHOS- and ET-states, thus making it possible to obtain flux control efficiencies.

2. Materials and methods

2.1. Reagents

Magnesium Green was purchased from Invitrogen/Thermo Fisher Scientific (cat. N° M3733). Antimycin A (cat. N° A8674), ATP (cat. N° A2383), CCCP (cat. N° C2759), malate (cat. N° M1000), $MgCl_2$ 1 M (cat. N° M1028), oligomycin (cat. N° O4876), pyruvate (cat. N° P2256), rotenone (cat. N° R8875), SF 6847 (cat. N° T182), and succinate (cat. N° S2378) were obtained from Sigma Aldrich. ADP was acquired from Millipore (cat. N° 117105), and carboxyatractyloside from Calbiochem (cat. N° 216201).

ADP and ATP were dissolved in deionized H_2O without addition of Mg^{2+} salts, pH was adjusted to 6.9 with KOH. Magnesium Green, malate, succinate, carboxyatractyloside and $MgCl_2$ were dissolved or diluted in deionized H_2O whereas antimycin A, CCCP, oligomycin, rotenone and SF 6847 were dissolved in ethanol p.a. All solutions were aliquoted and stored at $-20\text{ }^\circ\text{C}$, except pyruvate, which was dissolved in deionized H_2O fresh on the day of each experiment.

2.2. Animals

Wild-type C57BL/6N adult mice ($N=3$ per experimental group) were housed in the animal facility of the Medical University of Innsbruck (maximum 5 mice per cage) and maintained at $23\pm 3\text{ }^\circ\text{C}$, relative humidity 45–65 % with a controlled 12 h light/dark cycle in a conventional animal facility. Mice were fed *ad libitum* with free access to water. All procedures were conducted according to the Austrian Animal Experimentation Act in compliance with the European convention for the protection of vertebrate animals used for experimental and other scientific purposes (Tierversuchsgesetz 2012; Directive 2010/63/EU; BMWFM-66.011/0128-WF/V/3b/2016).

2.3. Cardiac mitochondrial isolation and protein concentration determination

Following cervical dislocation, the hearts were immediately excised and transferred into ice-cold biopsy preservation solution (BIOPS: 10 mM Ca²⁺-EGTA - 0.1 μM free Ca²⁺, 20 mM imidazole, 20 mM taurine, 50 mM K⁺-MES, 0.5 mM dithiothreitol, 6.56 mM MgCl₂, 5.77 mM ATP, 15 mM phosphocreatine, pH 7.1 adjusted with KOH) for short period of time (1–2 h; Fontana-Ayoub et al 2016). All procedures were performed on ice (Gnaiger et al 2000a). Mouse heart mitochondria were isolated following the protocol described by Fontana-Ayoub and Krumschnabel (2015). The heart (~ 80–120 mg) was washed to remove blood clots and minced with 1 mL of BIOPS. The tissue was homogenized with 2 mL isolation buffer (IB1: 0.5 M mannitol; 0.5 M sucrose; 0.1 M EGTA; pH 7.4 adjusted with Tris; 2.5 mg/mL BSA and 0.5 mg/mL subtilisin, the latter two added freshly on the day of use) in a 10 mL glass-Teflon Potter Elvehjem homogenizer, 6–8 × with about 1000 rpm mechanical rotation. 3 mL of IB1 was added to the homogenate which was centrifuged at 800 *g* for 10 min at 4 °C. The supernatant was centrifuged again, at 10 000 *g* for 10 min at 4 °C. The pellet was resuspended carefully using a 1 mL pipette in 0.5 mL IB2 (IB1 without subtilisin). After addition of 2 mL IB2, the homogenate was centrifuged again at 10 000 *g* for 10 min at 4 °C. The pellet was resuspended in 200 μL of IB3 (IB1 without BSA and subtilisin) and kept on ice until use on the same day within 2 h.

Protein concentration was used for calculation of mass specific O₂ flux, determined using the kit DC Protein Assay (Bio-Rad, Hercules, CA, US). Absorbance was measured at 620 nm with a Tecan Infinite TM F200 spectrophotometer (Tecan, Männedorf, Switzerland), using BSA at different concentrations as standards (Lowry et al 1951).

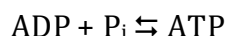
2.4. High-resolution respirometry

Oxygen consumption and ATP production measurements were performed simultaneously at 37 °C in the O2k-FluoRespirometer (O2k, Oroboros Instruments, Innsbruck, Austria). The O2k includes two Duran® glass chambers with stirring (750 rpm) and controlled temperature for closed-chamber respirometry using polarographic oxygen sensors (POS). Smart Fluo-Sensors Blue were used, with excitation LED 465 nm and filters for the LED and photodiode selected for Magnesium Green™). Specific amperometric emission and detection settings – fluorescence light intensity of 500 and gain 100 – were applied with the software DatLab 7.4 (Oroboros Instruments, Innsbruck, Austria) with continuous data recording set at 2 s time intervals. Standardized calibrations and instrumental O₂ background tests were performed (Doerrier et al 2018). The time-derivative of the O₂ concentration is calculated real-time by DatLab, providing traces of O₂ flux corrected for the O₂ instrumental background (Gnaiger 2001).

Experiments were run with cardiac isolated mitochondria at protein concentrations in the range of 0.026–0.049 mg/mL in modified mitochondrial respiration medium MiR05-MgG (MgCl₂ 1 mM instead of 3 mM in MiR05, EGTA 500 μM, KH₂PO₄ 10 mM, Hepes 20 mM, lactobionic acid 60 mM, D-sucrose 110 mM, taurine 20 mM, BSA 1 g/L, pH adjusted with KOH to 7.1). This modification of MiR05 (Gnaiger et al 2000a) was optimized for measurement of ATP production with MgG.

2.5. ATP production measurement with MgG

MgG (Magnesium Green™, pentapotassium salt, cell impermeant) does not permeate biological membranes. Therefore, the plasma membrane barrier function must be removed, as achieved in mitochondrial preparations – isolated mitochondria, tissue homogenates, permeabilized tissues and cells. MgG remains outside of the mitochondrial matrix and fluoresces when bound to Mg²⁺. In the phosphorylation reaction



reactants and MgG bind Mg²⁺ according to their apparent dissociation constants. When ADP is added to the experimental chamber, there is a fast drop of the fluorescence signal. If mitochondria and fuel substrates are present, ATP is generated and exchanged with ADP by the ANT. ATP has a higher affinity to Mg²⁺ compared to ADP. As ATP concentration increases in the medium, the free Mg²⁺ concentration declines, less MgG is bound to Mg²⁺, and the fluorescence decreases. After calibration of the fluorescence signal in terms of free [Mg²⁺], ATP concentration in the medium is calculated according to Chinopoulos et al (2009; 2014), taking in account that: (1) the initial concentration of ATP is zero, (2) the initial concentration of ADP is known, (3) the concentration of Mg²⁺ is measured, and (4) apparent K_d values for ADP and ATP with Mg²⁺ are obtained experimentally.

The free Mg²⁺ concentration was calibrated in MiR05-MgG containing the mitochondrial sample, fuel substrates, carboxyatractyloside, and oligomycin. MgCl₂ was titrated in 10 steps of 0.1 mM to obtain a non-linear fit for calibration of the amperometric signal converted from current to voltage U (free [Mg²⁺] = $(a \times U^2) + (b \times U) + c$) (Chinopoulos et al 2014). After calibration, the apparent K_d (K_d') of ADP and ATP for Mg²⁺ was determined for each experimental condition by performing multiple titrations with ADP or ATP. To test for an influence of EGTA on the MgG calibration, similar calibrations and K_d' determination curves were performed in the absence of sample, fuel substrates, and with varying EGTA concentrations in the range of 5 – 500 μM.

2.6. Substrate-uncoupler-inhibitor-titration (SUIT) protocols

Coupling control protocols (SUIT-006) assess different coupling control states – LEAK, OXPHOS and ET – at a constant ET-pathway state (Gnaiger et al 2020). The effect of MgG on mitochondrial respiration was evaluated by adding 1.1 μM MgG to the experimental chamber prior to sample addition, but not to the controls which were maintained at an identical fluorescence light intensity. Since the fluorescent dye was diluted in water and a volume of only 2 μL was added into the 2 mL chamber, no solvent addition was performed in the control group without MgG. After addition of mitochondria into the O2k chambers, residual oxygen consumption R_{ox} was measured in the absence of substrates. Two coupling-control protocols were used to study simultaneously oxygen consumption and ATP production with the following titrations: NADH-pathway with 5 mM pyruvate and 2 mM malate, or Succinate-pathway with 0.5 μM rotenone and 10 mM succinate. First, LEAK respiration was measured in the absence of ADP. Second, OXPHOS capacity was measured after addition of 2 mM ADP. Oligomycin (7.5–10.0 nM) or carboxyatractyloside (0.3 – 0.4 mM) were added to induce again a LEAK state. Both inhibitors have the same function in the context of the present experiments, to induce

LEAK respiration by inhibition of the phosphorylation system. This was followed by stepwise titration of uncouplers up to the optimum concentration, when the maximum O₂ flux was achieved as a measure of ET capacity. CCCP (0.5 μM steps) or SF 6847 (25–50 nM steps) were used. Both protonophores have the same function. Finally, *Rox* was measured after addition of the CIII inhibitor antimycin A (2.5 μM). The fluorescence signal in the control group did not change on the scale used to analyze the MgG data, such that corrections for changes of autofluorescence were not required.

2.7. Data analysis

The assays were repeated 3 times with independent mitochondrial preparations, with or without MgG, for each condition tested. Data analysis for O₂ consumption, calculations of K_d' and ATP production following Chinopoulos et al 2014, were performed using the templates provided with the software DatLab 7.4.

3. Results and discussion

To determine ATP production and respiration, a variation of the MiR05 medium was prepared without EGTA nor MgCl₂, which were titrated during the calibrations. EGTA is used to chelate Ca²⁺ ions that could affect mitochondrial function. In addition, free Ca²⁺ affects the MgG assay since this fluorophore has a higher affinity for Ca²⁺ than Mg²⁺ (Molecular Probes 2005).

The chemicals used to prepare the media may contain contaminations. Titration of KH₂PO₄ increased fluorescence of MgG, which was decreased upon addition of EGTA (not shown). With a low concentration of EGTA (5 μM), it was not possible to chelate all contaminants, as shown by the lower signal after titration of ADP or ATP (in the presence of 1 mM MgCl₂) compared to the signal before MgCl₂ titration, thus making it impossible to determine the K_d' values (Figure 1a and b). 50 μM EGTA was needed (Figure 1c and d), with similar results at 500 μM EGTA (Figure 1e and f). The K_d' of ADP³⁻-Mg²⁺ and ATP⁴⁻-Mg²⁺ determined in the presence of 50 μM or 500 μM EGTA were not different (Figure 1g and h).

Even though 500 μM EGTA partially chelates Mg²⁺ in the medium, this EGTA concentration did not interfere with the calibrations of MgG (Figure 1e and f). Therefore, 500 μM EGTA was selected to foster a higher capacity for binding contaminating cations under experimental conditions in the presence of mitochondria. With the modified MiR05 (1 mM MgCl₂), titration of 2 mM ADP leads to binding of ~ 60 % of the initial free Mg²⁺. Even if 500 μM EGTA is mostly bound as EGTA-Mg²⁺, still 0.5 mM Mg²⁺ would be free before ADP titration, and a minimum of ~ 0.19 mM would be free upon titration of 2 mM ADP. Under our experimental conditions, the free Mg²⁺ was sufficient to monitor the further decrease in MgG fluorescence over time due to ATP production (Figures 3b and 4b). As shown by Chinopoulos et al (2009), too low concentrations of free Mg²⁺ decrease the signal-to-noise ratio. Media with 500 μM EGTA and 3 mM MgCl₂ have been used to determine ATP production using MgG (Pham et al 2014, Devaux et al 2019). However, with 3 mM MgCl₂, the decrease in the signal upon titration of ADP or ATP is lower, such that 1 mM MgCl₂ was considered to be optimum.

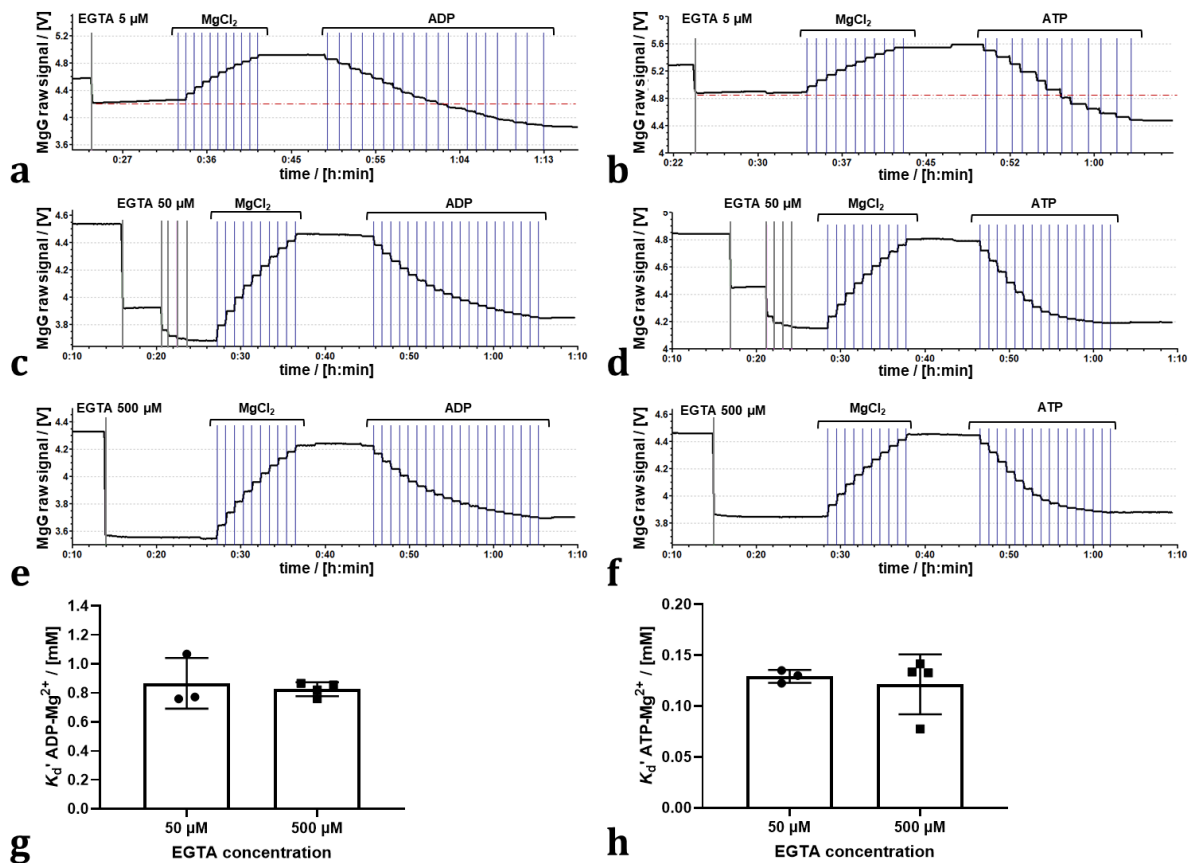


Figure 1. Effect of EGTA concentration on K_d' of ADP³⁻-Mg²⁺ and ATP⁴⁻-Mg²⁺: Representative traces of calibration in MiR05 (10 titrations of 0.1 mM MgCl₂ by TIP2k) and titrations of (a, c, e) ADP (0.25 mM/titration) or (b, d, f) ATP (0.20 mM/titration), in the presence of 5, 50 (5 titrations of 10 μM EGTA) or 500 μM EGTA. (g, h) K_d' for ADP³⁻-Mg²⁺ or ATP⁴⁻-Mg²⁺ determined in the presence of 50 or 500 μM EGTA. Dots represent independent measurements; bars represent average and standard deviation. No statistical difference was found ($p > 0.05$; Welch's t-test).

Figures 3a and 4a show superimposed traces of O₂ concentration and O₂ flux per mass. Coupling control of mitochondrial respiration was measured in two different electron-transfer-pathway control states. In the N-protocol, the NADH-linked pathway through Complex I (CI) was evaluated in the presence of pyruvate and malate which stimulate dehydrogenases of the TCA cycle, leading to reduction of NAD⁺ to NADH. NADH is the substrate of CI, with further electron flow into the Q-junction, CIII and CIV (Figure 2). In the S-protocol, CI was inhibited by rotenone to prevent reverse electron transfer and accumulation of oxaloacetate, which is an inhibitor of succinate dehydrogenase (Makrecka-Kuka et al 2015; Gnaiger 2020), and respiration was measured supported by succinate as the substrate of CII (Figure 3).

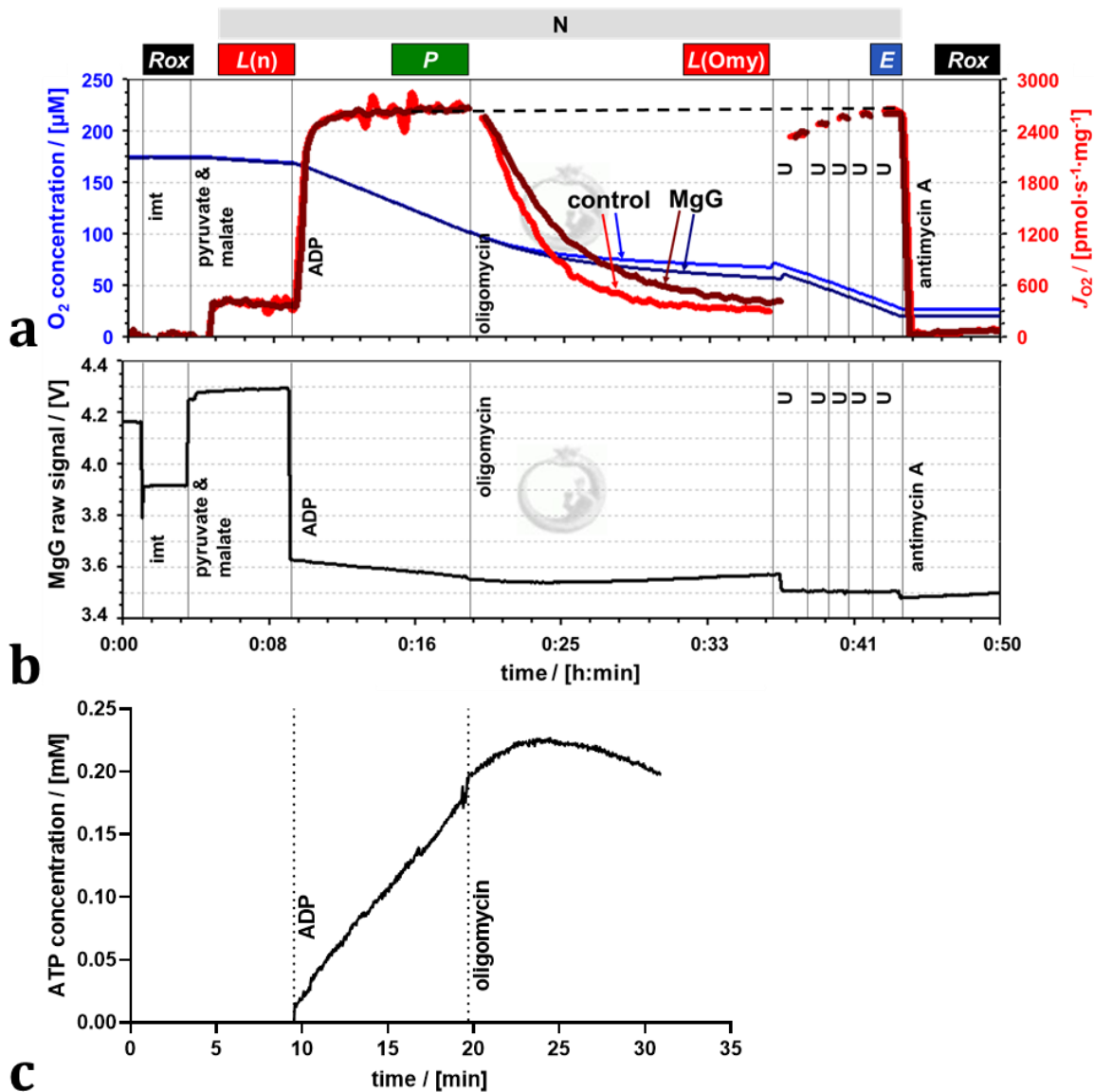


Figure 2. Simultaneous measurement of respiration and ATP production by high-resolution Fluorespirometry in mitochondria isolated from mouse heart. Representative traces for coupling control protocol SUIT-006 with NADH-linked substrates (N-protocol), following additions (respiratory states): isolated mitochondria imt (ROX), pyruvate & malate (LEAK), ADP (OXPHOS), oligomycin (LEAK), uncoupler U (ET), and antimycin A (ROX). Experiment 2019-02-07 P5 04: **(a)** O₂ concentration (dark and lighter blue traces) and O₂ flux per mass (dark and lighter red), 1.1 μM MgG versus control; **(b)** MgG fluorescence signal; **(c)** ATP concentration calculated from MgG signal calibrated as Mg²⁺ concentration.

In both protocols, LEAK respiration was measured (1) *L(n)*, in the absence of adenylates and (2) *L(Omy)* or *L(Cat)*, in the presence of phosphorylation system inhibitors. Respiration in these two LEAK states was similar, but slightly lower in *L(Omy)* with the N-protocol (Figure 2a, Table 1). *L(n)* stabilized quickly, whereas for *L(Omy)*

inhibition of respiration was slow at the low concentration of 7.5–10.0 nM oligomycin. In the S-protocol with sequential addition of rotenone followed by succinate, $L(n)$ increased for a few minutes until stabilization (Figure 3a). Inhibition by carboxyatractyloside (0.3–0.4 μM) was immediate, and $L(\text{Cat})$ tended to be slightly lower than $L(n)$ (Table 1).

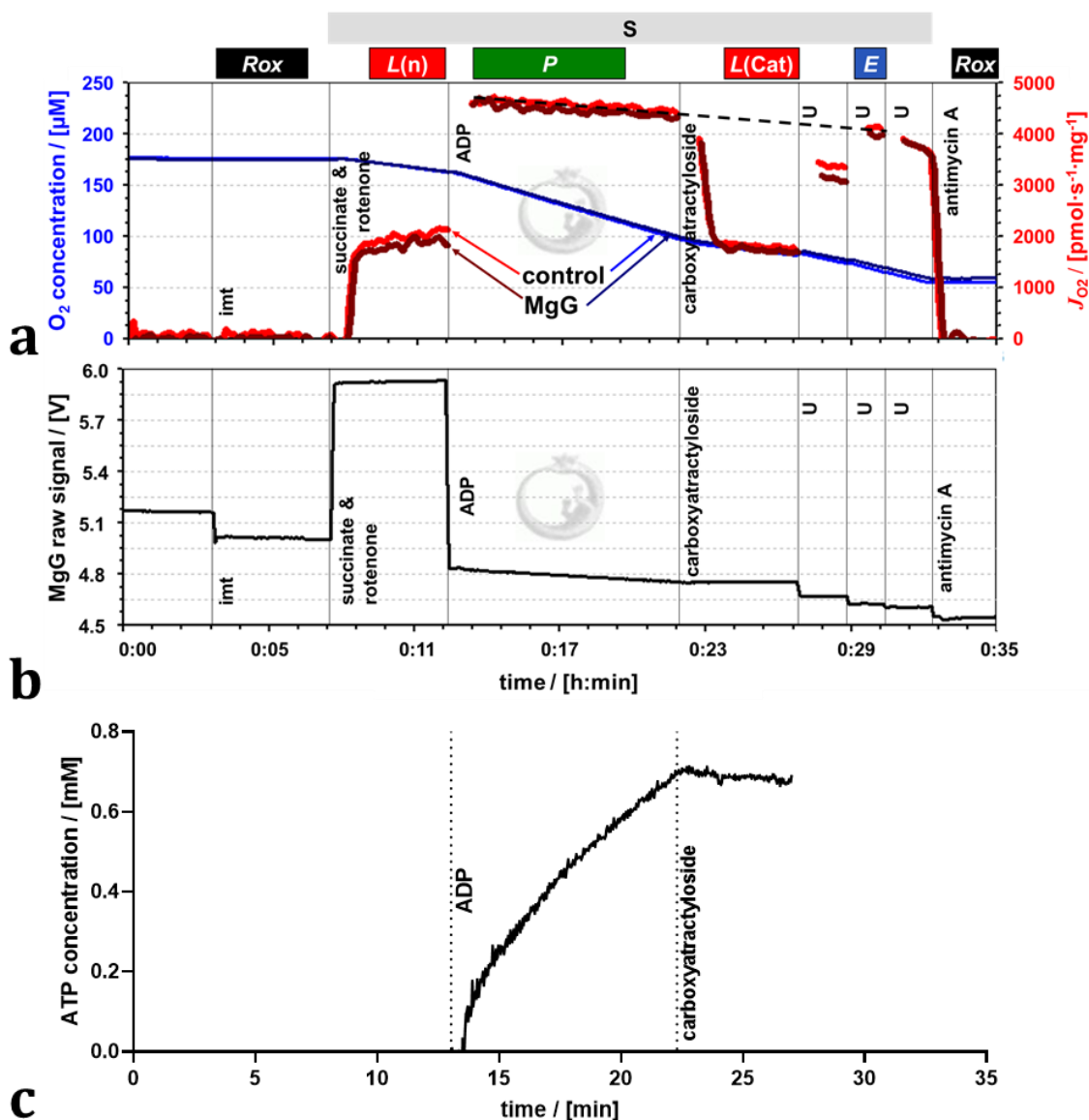


Figure 3. Simultaneous measurement of respiration and ATP production by high-resolution Fluorespirometry in mitochondria isolated from mouse heart. Representative traces for coupling control protocol SUIT-006 with succinate as substrate (S-protocol), following additions (respiratory states): isolated mitochondria imt (ROX), succinate & rotenone (LEAK), ADP (OXPHOS), carboxyatractyloside (LEAK), uncoupler U (ET), and antimycin A (ROX). Experiment 2019-03-18 P5-03: **(a)** O_2 concentration (dark and lighter blue traces) and O_2 flux per mass (dark and lighter red), 1.1 μM MgG versus control; **(b)** MgG fluorescence signal; **(c)** ATP concentration calculated from MgG signal calibrated as Mg^{2+} concentration.

Table 1. Coupling control efficiency ($P-L$)/ P and $P\gg/O_2$ ratio in absence or presence of MgG. Average \pm SD, $N=3$. OXPHOS capacity P and LEAK respiration L corrected for residual oxygen consumption R_{ox} . $L(n)/L(inh)$ ratios: L in the absence of adenylates (n) over L with an inhibitor (inh) of the phosphorylation system, oligomycin Omy or carboxyatractyloside Cat for the N- or S-pathway, respectively. $L(inh)$ is used in $(P-L)/P$.

Protocol	$(P-L)/P$	$L(n)/L(inh)$	$P\gg/O_2$	$P\gg/O$
N-pathway - MgG	0.90 ± 0.01	1.13 ± 0.05	-	-
N-pathway + MgG	0.88 ± 0.02	1.12 ± 0.04	2.33 ± 1.07	1.16 ± 0.53
S-pathway - MgG	0.62 ± 0.05	1.27 ± 0.16	-	-
S-pathway + MgG	0.61 ± 0.05	1.12 ± 0.26	2.78 ± 0.74	1.39 ± 0.37

OXPHOS capacity P was measured in the presence of a kinetically saturating concentration of ADP. The optimum uncoupler concentrations to measure maximum ET capacity E were 6.0–7.0 μ M CCCP in the N-protocol, and 0.150–0.175 μ M SF 6847 in the S-protocol. In the N-protocol, P was stable over time and identical to E . However, in the S-protocol, P showed a slight decrease over time. Extrapolating this trend of declining O₂ flux to the point where ET capacity was measured explains why E appears to be lower than P (dashed trendline, Figure 3a). In both protocols, therefore, $E = P$, indicating that OXPHOS capacity was not limited by the phosphorylation system. This agrees with results for mouse heart mitochondria on coupling control even in the combined NS-pathway (Lemieux et al 2017). Parallel measurements were performed in the presence and absence of 1.1 μ M MgG with the N- and S-protocol. This low concentration of MgG is sufficiently high for calculating ATP production (Figures 3b and c and Figures 4b and c).

The MgG assay to measure ATP production can be used concomitantly with high-resolution respirometry, providing information real-time. Other methods are available to detect ATP production real-time. Spectrophotometric detection of NADPH can be used in conjunction with the coupled enzyme system hexokinase and glucose-6-phosphate dehydrogenase (Horgan, 1978). This assay has been adapted for simultaneous detection of O₂ consumption and NADPH (Lark et al 2016). The luciferin/luciferase assay can be used for continuous measurement of ATP production (Manfredi et al 2002). It is important to note that luciferase consumes O₂, and instruments typically used for luminometry do not allow monitoring of O₂ concentration in parallel.

Another method for continuous measurement of the $P\gg/O_2$ ratio is the steady-state ADP injection-respirometry (Gnaiger et al 2000b; 2001). The phosphorylation rate is set by continuous injection of ADP as the rate-limiting step while measuring O₂ consumption stimulated to a constant sub-maximal level. Chance and Williams (1955) originally described a polarographic ADP pulse-titration method to determine the $P\gg/O_2$ ratio, titrating a known concentration of ADP, which leads to a peak of O₂ consumption stimulated by the complete phosphorylation of ADP to ATP. The ADP pulse-titration method has been extended and critically discussed by Gnaiger (2001).

End-point assays are available to detect ATP levels, providing discontinuous measurement of ATP production. These include chromatography (high performance liquid chromatography, HPLC; thin layer chromatography, TLC); nuclear magnetic

resonance detection of 2-deoxyglucose and its phosphorylated form, and radioactivity measurements using ^{32}P (Menegollo et al 2019; Morciano et al 2017; Fink et al 2017; Sausen et al 2019).

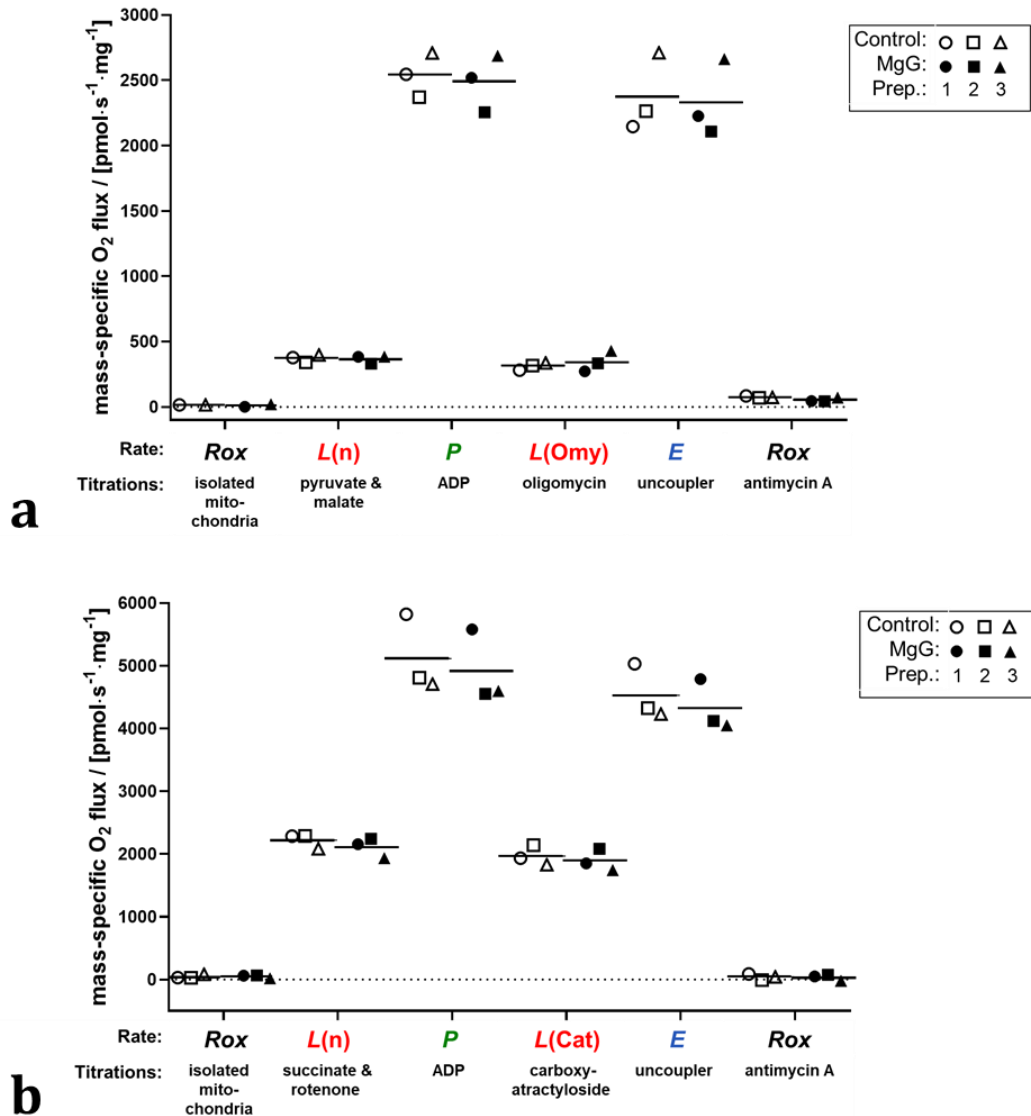


Figure 4. O₂ consumption in the absence and presence of MgG by mitochondria isolated from mouse heart. The respiratory rates indicated in the abscissa were measured by HRR with two coupling control protocols SUIT-006, with the following respiratory states: ROX, LEAK (in the absence of adenylates), OXPHOS, LEAK (in the presence of inhibitors), ET, and ROX. Sequential titrations are described for **(a)** N-protocol (experiments 2019-02-05 P3-04, 2019-02-06 P3-03 and 2019-02-07 P5-04) and **(b)** S-protocol (experiments 2019-03-13 P6-03, 2019-03-14 P3-03 and 2019-03-18 P5-03). For both graphs the three symbol shapes show independent mitochondrial preparations (prep.), whereas open and closed symbols compare results in controls and in the presence of MgG from the same preparation; bars represent the average.

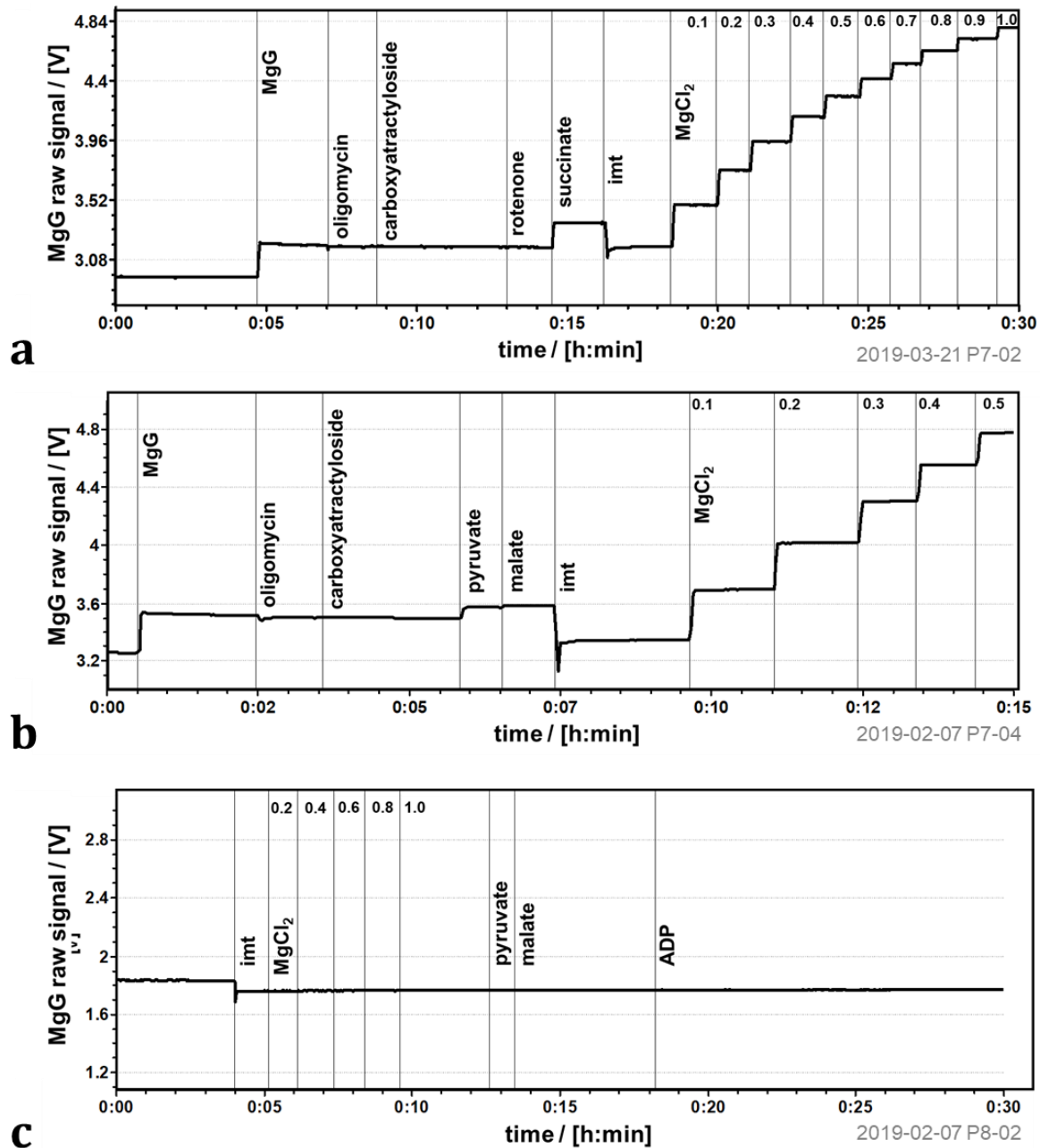


Figure 5. Chemical background signal with MgG. MiR05 (without MgCl₂) in the absence of sample, and titrations as indicated in the figure. Note the increase in fluorescence upon titration of **(a)** succinate and **(b)** pyruvate, despite dilution of the MgG by 1 % and 0.25% respectively. Titration of mitochondria isolated from mouse heart (imt) leads to change in optical properties and decreases the signal in the **(a, b)** presence and **(c)** absence of MgG. Calibration with MgCl₂ [mM].

The fluorometric MgG assay applied simultaneously with O₂ consumption by HRR has been used extensively (Iftikar, Hickey 2013; Goo et al 2013; Chinopoulos et al 2014; Pham et al 2014; Power et al 2014; Salin et al 2016; Napa et al 2017; Masson et al 2017;

Salin et al 2018; Devaux et al 2019; Salin et al 2019). Understanding whether MgG may affect respiration is crucial for such studies, particularly for P_{\gg}/O_2 ratios obtained in different electron-transfer-pathway states.

It is well established that different dyes commonly applied to measure mitochondrial membrane potential inhibit OXPHOS capacity, *e.g.*, safranin, rhodamine 123 and its derivatives TMRM and TMRE (Krumshnabel et al 2014; Scaduto, Grotyohann 1999). Surprisingly, Amplex UltraRed used to detect H_2O_2 flux impairs respiration despite not accumulating in the mitochondria (Makrecka-Kuka et al 2015). Therefore, we studied the effect of MgG on respiration. MgG at 1.1 μM did not affect NADH-linked nor succinate-linked respiration in any coupling control state (LEAK, OXPHOS and ET) measured in mitochondria isolated from mouse hearts (Figure 4). In addition, residual oxygen consumption was not affected by MgG. Similar controls should be applied in studies of mitochondria from other species and tissues or cells, and under different experimental conditions including media with different composition and different MgG concentrations.

Addition of succinate and pyruvate in the absence of sample resulted in a chemical background effect (Figure 5a and b). A similar increase of fluorescence was seen after titration of succinate or pyruvate in the presence of isolated mitochondria (Figures 4b and 3b), which is therefore explained by the chemical background. This enforces the recommendation of obtaining the K_d' for $ATP^{4-}\text{-Mg}^{2+}$ and $ADP^{3-}\text{-Mg}^{2+}$ in the presence of the substrates used in the reaction media, as discussed previously (Chinopoulos et al 2014). The addition of sample leads to a decrease in the amperometric signal both in the chambers with and without MgG (Figure 5a, b and c), indicating that this effect is at least partly due to shadowing/blocking the light. The intensity of this signal change varies, as well as the initial MgG signal might vary. Therefore, it is advisable to perform a calibration with each sample tested under the same experimental conditions (same batches of media, chemicals and MgG, in the same instrumental chamber used).

The NADH-pathway has three coupling sites, CI, CIII and CIV, whereas the succinate-pathway has only the latter two, resulting in a lower P_{\gg}/O_2 ratio. When dividing ATP flux, calculated from the increase in ATP concentration over time, by the simultaneously measured O_2 flux, then P_{\gg}/O_2 flux ratios ($J_{P_{\gg}}/J_{O_2}$) are obtained. The P_{\gg}/O_2 is twice the classical P_{\gg}/O (Table 1). P_{\gg}/O_2 obtained for the S-pathway was close to the theoretically expected value (Gnaiger et al 2020). The result obtained for the N-pathway was lower than expected. A limitation of the present study is the low number of replicates ($N = 3$), with a high variability of P_{\gg}/O_2 ratios. Further experiments are necessary to investigate and compare P_{\gg}/O_2 ratios, which is beyond the aim of this technical communication.

Coupling control efficiencies are closely related to P_{\gg}/O_2 ratios. The coupling control efficiency is defined as $(E-L)/E$, ranging from 0, at zero coupling, to 1 in a fully coupled system. In the present case of $P = E$, the coupling control efficiency is expressed as the $P-L$ control efficiency, $(P-L)/P$ (Gnaiger 2020). As expected, a higher $P-L$ control efficiency of 0.89 ± 0.02 was found for the N-pathway than 0.62 ± 0.05 for the S-pathway (pooled data with and without MgG, average \pm standard deviation, $N = 6$; Table 1). These correspond to a RCR = P/L of 9.6 ± 1.8 for the N-pathway and 2.6 ± 0.3 for the S-pathway.

In summary, MgG did not affect respiration in any of the coupling control states. These results demonstrate that measurement of O₂ consumption is reliable concomitant with the MgG assay in SUIT protocols with different pathway states and coupling states.

Acknowledgements

We thank Marco Di Marcello and Manuela Passrigger for expert technical support on media and chemicals preparation, equipment maintenance and mitochondria isolation, Cristiane Cecatto for discussions on autofluorescence corrections, and the BEC reviewers for helpful suggestions. This work was partially funded by the European Union's Horizon 2020 research and innovation programme under grant agreement No. 859770, NextGen-O2k project. An initiative of the MitoEAGLE Task Group of the Mitochondrial Physiology Society.

Abbreviations

Amp amperometric; ANT adenosine nucleotide translocase; BSA bovine serum albumin; CI to CIV Complex I to IV; CCCP carbonyl cyanide *m*-chlorophenyl hydrazine; $\Delta\Psi_{p+}$ mt-membrane potential; EGTA ethylene glycol tetraacetic acid; *E* ET capacity; ETS electron transfer system; F₀F₁ ATP synthase; Hepes *N*-(2-hydroxyethyl)piperazine-*N'*-(2-ethanesulfonic acid); HRR high-resolution respirometry; imt isolated mitochondria; *J*_{O₂} O₂ flux; *K*_d dissociation constant; *K*_d' apparent *K*_d; *L* LEAK respiration; LED light-emitting diode; MES 2-(*N*-morpholino)ethanesulfonic acid hydrate; MgG Magnesium Green; *P* OXPHOS capacity; P_»/O ADP phosphorylated per atom oxygen consumed; P_»/O₂ ADP phosphorylated per molecular oxygen consumed; P_i inorganic phosphate; RCR respiratory acceptor control ratio; *Rox* residual oxygen consumption; SUIT substrate-uncoupler -inhibitor-titration; TCA tricarboxylic acid; TMRM tetramethylrhodamine methyl ester; TMRE tetramethylrhodamine ethyl ester; TPP⁺ tetraphenylphosphonium; Tris 2-amino-2-(hydroxymethyl)-1,3-propanediol; U uncoupler.

References

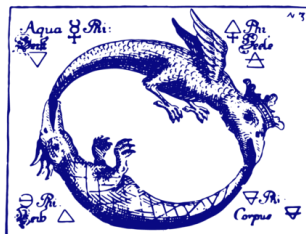
- Budinger GRS, Duranteau J, Chandel NS, Schumacker PT (1998) Hibernation during hypoxia in cardiomyocytes. Role of mitochondria as the O₂ sensor. *J Biol Chem* 273:3320-6.
- Chance B, Williams GR (1955) Respiratory enzymes in oxidative phosphorylation. I. Kinetics of oxygen utilization. *J Biol Chem* 217:383-93.
- Chinopoulos C, Vajda S, Csanady L, Mandi M, Mathe K, Adam-Vizi V (2009) A Novel Kinetic Assay of Mitochondrial ATP-ADP Exchange Rate Mediated by the ANT. *Biophys J* 96:2490-504.
- Chinopoulos C, Kiss G, Kawamata H, Starkov AA (2014) Measurement of ADP-ATP exchange in relation to mitochondrial transmembrane potential and oxygen consumption. *Methods Enzymol* 542:333-48.
- Devaux JBL, Hedges CP, Birch N, Herbert N, Renshaw GMC, Hickey AJR (2019) Acidosis maintains the function of brain mitochondria in hypoxia-tolerant triplefin fish: a strategy to survive acute hypoxic exposure? *Front Physiol* 9:1941.
- Doerrier C, Garcia-Souza LF, Krumschnabel G, Wohlfarter Y, Mészáros AT, Gnaiger E (2018) High-Resolution FluoRespirometry and OXPHOS protocols for human cells, permeabilized fibers from small biopsies of muscle, and isolated mitochondria. *Methods Mol Biol* 1782:31-70.
- Fink BD, Bai F, Yu L, Sivitz WI (2017) Regulation of ATP production: dependence on calcium concentration and respiratory state. *Am J Physiol Cell Physiol* 313:C146-53.
- Fontana M, Krumschnabel G (2015) Isolation of mouse heart mitochondria. *Mitochondr Physiol Network* 20.06(01):1-2.

- Fontana-Ayoub M, Fasching M, Gnaiger E (2016) Selected media and chemicals for respirometry with mitochondrial preparations. *Mitochondr Physiol Network* 03.02(18):1-10.
- Gnaiger E, Wyss M (1994) Chemical forces in the cell: Calculation for the ATP system. In: *What is Controlling Life?* (Gnaiger E, Gellerich FN, Wyss M, eds) *Modern Trends in BioThermoKinetics* 3. Innsbruck Univ Press:207-12.
- Gnaiger E (2001) Bioenergetics at low oxygen: dependence of respiration and phosphorylation on oxygen and adenosine diphosphate supply. *Respir Physiol* 128:277-97.
- Gnaiger E (2020) Mitochondrial pathways and respiratory control. An introduction to OXPHOS analysis. 5th ed. *Bioenerg Commun* 2020.2: 112 pp. doi:10.26124/bec:2020-0002.
- Gnaiger E et al – MitoEAGLE Task Group (2020) Mitochondrial physiology. *Bioenerg Commun* 2020.1. doi:10.26124/bec:2020-0001.v1.
- Gnaiger E, Kuznetsov AV, Schneeberger S, Seiler R, Brandacher G, Steurer W, Margreiter R (2000a) Mitochondria in the cold. In: *Life in the Cold* (Heldmaier G, Klingenspor M, eds) Springer, Heidelberg, Berlin, New York:431-42.
- Gnaiger E, Méndez G, Hand SC (2000b) High phosphorylation efficiency and depression of uncoupled respiration in mitochondria under hypoxia. *Proc Natl Acad Sci U S A* 97:11080-5.
- Goo S, Pham T, Han JC, Nielsen P, Taberner A, Hickey A, Loiselle D (2013) Multiscale measurement of cardiac energetics. *Clin Exp Pharmacol Physiol* 40:671-81.
- Horgan DJ (1978) A spectrophotometric assay of ATP synthesized by sarcoplasmic reticulum. *Aust J Biol Sci* 31:21-4.
- Iftikar FI, Hickey AJ (2013) Do mitochondria limit hot fish hearts? Understanding the role of mitochondrial function with heat stress in *Notolabrus celidotus*. *PLoS One* 8:e64120.
- Krumschnabel G, Eigentler A, Fasching M, Gnaiger E (2014) Use of safranin for the assessment of mitochondrial membrane potential by high-resolution respirometry and fluorometry. *Methods Enzymol* 542:163-81.
- Lark DS, Torres MJ, Lin CT, Ryan TE, Anderson EJ, Neuffer PD (2016) Direct real-time quantification of mitochondrial oxidative phosphorylation efficiency in permeabilized skeletal muscle myofibers. *Am J Physiol Cell Physiol* 311:C239-45.
- Lemieux H, Blier PU, Gnaiger E (2017) Remodeling pathway control of mitochondrial respiratory capacity by temperature in mouse heart: electron flow through the Q-junction in permeabilized fibers. *Sci Rep* 7:2840, DOI:10.1038/s41598-017-02789-8.
- Leyssens A, Nowicky AV, Patterson L, Crompton M, Duchon MR (1996) The relationship between mitochondrial state, ATP hydrolysis, $[Mg^{2+}]_i$ and $[Ca^{2+}]_i$ studied in isolated rat cardiomyocytes. *J Physiol* 496:111-28.
- Lowry OH, Rosebrough NJ, Farr AL, Randall RJ (1951) Protein measurement with the Folin phenol reagent. *J Biol Chem* 193:265-275.
- Makrečka-Kuka M, Krumschnabel G, Gnaiger E (2015) High-resolution respirometry for simultaneous measurement of oxygen and hydrogen peroxide fluxes in permeabilized cells, tissue homogenate and isolated mitochondria. *Biomolecules* 5:1319-38.
- Manfredi G, Yang L, Gajewski CD, Mattiazzi M (2002) Measurements of ATP in mammalian cells. *Methods* 26:317-26.
- Masson SWC, Hedges CP, Devaux JBL, James CS, Hickey AJR (2017) Mitochondrial glycerol 3-phosphate facilitates bumblebee pre-flight thermogenesis. *Sci Rep* 7:13107.
- Menegollo M, Tessari I, Bubacco L, Szabadkai G (2019) Determination of ATP, ADP, and AMP Levels by Reversed-Phase High-Performance Liquid Chromatography in Cultured Cells. *Methods Mol Biol* 1925:223-32.
- Molecular Probes. Fluorescent Magnesium Indicators. Revised: 05-May-2005. Available online at: <https://assets.thermofisher.com/TFS-Assets/LSG/manuals/mp01290.pdf>
- Morciano G, Sarti AC, Marchi S, Missiroli S, Falzoni S, Raffaghello L, Pistoia V, Giorgi C, Di Virgilio F, Pinton P (2017) Use of luciferase probes to measure ATP in living cells and animals. *Nat Protoc* 12:1542-62.
- Napa K, Baeder AC, Witt JE, Rayburn ST, Miller MG, Dallon BW, Gibbs JL, Wilcox SH, Winden DR, Smith JH, Reynolds PR, Bikman BT (2017) LPS from *P. gingivalis* negatively alters gingival cell mitochondrial bioenergetics. *Int J Dent* 2017:2697210.

- Pham T, Loiselle D, Power A, Hickey AJ (2014) Mitochondrial inefficiencies and anoxic ATP hydrolysis capacities in diabetic rat heart. *Am J Physiol* 307:C499–507.
- Power A, Pearson N, Pham T, Cheung C, Phillips A, Hickey A (2014) Uncoupling of oxidative phosphorylation and ATP synthase reversal within the hyperthermic heart. *Physiol Rep* pii:e12138.
- Salin K, Villasevil EM, Auer SK, Anderson GJ, Selman C, Metcalfe NB, Chinopoulos C (2016) Simultaneous measurement of mitochondrial respiration and ATP production in tissue homogenates and calculation of effective P/O ratios. *Physiol Rep* 10.14814/phy2.13007.
- Salin K, Villasevil EM, Anderson GJ, Selman C, Chinopoulos C, Metcalfe NB (2018) The RCR and ATP/O indices can give contradictory messages about mitochondrial efficiency. *Integr Comp Biol* 58:486-94.
- Salin K, Villasevil EM, Anderson GJ, Lamarre SG, Melanson CA, McCarthy I, Selman C, Metcalfe NB (2019) Differences in mitochondrial efficiency explain individual variation in growth performance. *Proc Biol Sci* 286:20191466.
- Sausen CW, Rogers CM, Bochman ML (2019) Thin-Layer Chromatography and Real-Time Coupled Assays to Measure ATP Hydrolysis. *Methods Mol Biol* 1999:245-253.
- Scaduto RC Jr, Grotyohann LW (1999) Measurement of mitochondrial membrane potential using fluorescent rhodamine derivatives. *Biophys J* 76:469-77.



Copyright © 2021 The authors. This Open Access peer-reviewed communication is distributed under the terms of the Creative Commons Attribution License, which permits unrestricted use, distribution, and reproduction in any medium, provided the original authors and source are credited. © remains with the authors, who have granted BEC an Open Access publication license in perpetuity.



BIOENERGETICS
COMMUNICATIONS